

POSITRON TRANSMISSION AND POLARIZATION IN E-166 EXPERIMENT*

Yuri K. Batygin, SLAC, Stanford, CA 94309, USA

Abstract

The proposed experiment E-166 at SLAC is designed to demonstrate the possibility of producing longitudinally polarized positrons from circularly polarized photons. The experimental set-up utilizes a low emittance 50 GeV electron beam passing through a helical undulator in the Final Focus Test Beam line of the SLAC accelerator. Circularly polarized photons generated by the electron beam in the undulator hit a target and produce electron-positron pairs. The purpose of the post-target spectrometer is to select the positron beam and to deliver it to a polarimeter, keeping the positron beam polarization as high as possible. The paper analyzes the positron transmission and polarization in the E-166 spectrometer both numerically and analytically. The value of positron transmission has a maximum of 5% for positron energy of 7 MeV, while positron polarization is around 80%.

INTRODUCTION

The polarized positron production experiment E-166 uses a strongly collimated 50 GeV electron beam to generate circularly polarized photons in a helical undulator. Photons, after interaction with a target, create polarized positrons. The layout and general description of experiment are given in Ref. [1]. The purpose of a spectrometer is to select the positron beam after the target from electron and photon beams and to deliver positrons to a reversion target, keeping beam polarization as high as possible.

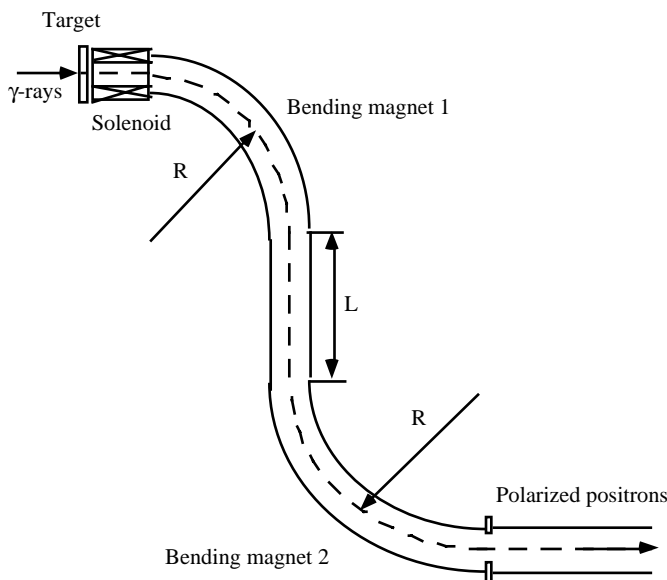


Figure 1: Layout of spectrometer.

Table 1: Parameters of spectrometer

Positron beam energy	0..10 MeV
Bending radius, R	12.5 cm
Bending angle, θ	90°
Drift space, L	20 cm
Positron transmission	5%
Positron polarization	80%

POLARIZED POSITRON DISTRIBUTION AFTER TARGET

The initial distribution of positrons produced by circularly polarized photons was calculated by J.C.Sheppard using the program EGS4, modified for polarized positrons [2, 3]. Positron distribution after the target is presented in Fig. 2. The distribution is characterized by a large emittance of the positron beam and a large energy spread. The correlation between energy, polarization, and transverse momentum spread is illustrated by partial distributions presented in Figs. 3 – 5. Low energy positrons are less polarized and more transversely divergent, while high-energy positrons are strongly polarized and less divergent. The energy spectrum peaks near the low-energy end of the distribution.

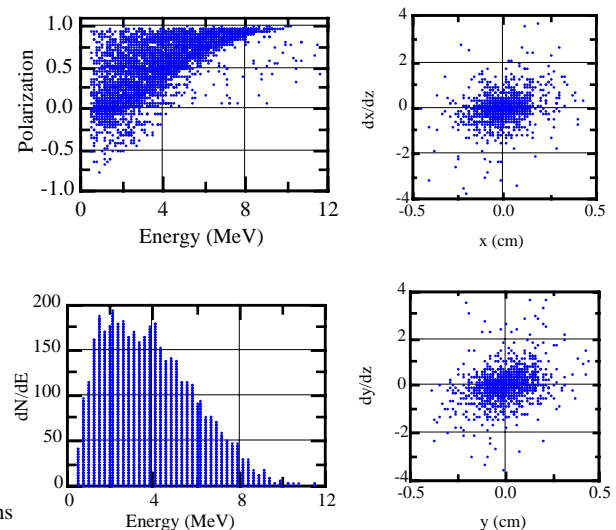


Figure 2: Initial distribution of positrons.

*Work is supported by Department of Energy under Contract No. DE-AC03-76SF00515

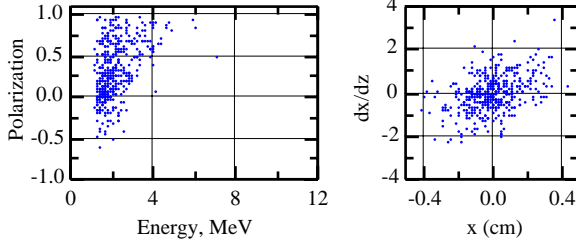


Figure 3: Fraction of initial positron distribution with average energy of $\bar{E} = 1.9$ MeV, and $\Delta E/\bar{E} = \pm 0.15$.

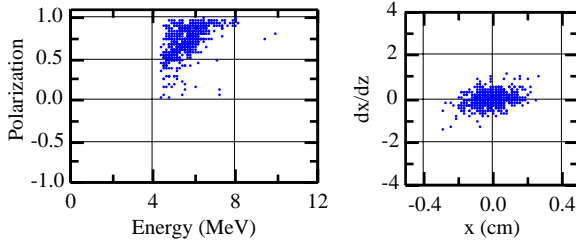


Figure 4: Fraction of initial positron distribution with average energy of $\bar{E} = 5.3$ MeV, and $\Delta E/\bar{E} = \pm 0.15$.

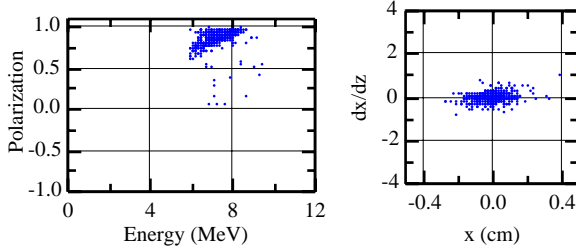


Figure 5: Fraction of initial positron distribution with average energy of $\bar{E} = 7.5$ MeV, and $\Delta E/\bar{E} = \pm 0.15$.

SPECTROMETER WITH DOUBLE 90° MAGNETS

In the proposed experiment E-166, the spectrometer has to shift the beam from an original accelerator axis at the distance of 45 cm to separate the positron beam from a photon beam and an electron beam coming out from the target. The simple and cost-effective solution is to utilize two 90° magnets providing a point-to-point transformation of the beam (see Fig. 6). The spectrometer includes a focusing solenoid and two 90° bending magnets separated by a drift space of $L = 20$ cm.

From the first order matrix analysis, the horizontal displacement of the particle after the first bend and drift is given by:

$$x = -\frac{L}{R} x_0 + R x_0' + (R+L) \frac{\Delta p}{p_0}. \quad (1)$$

The maximum deviation from the axis is equal to the radial aperture, $a_x = 5$ cm. Maximum radial displacement is $x_{0, \max} = a_x R/L = 3.125$ cm and maximum divergence is

$x_{0, \max}' = a_x/R = 0.4$. Therefore, horizontal acceptance of the channel, ϵ_x , is defined as:

$$\epsilon_x = \pi x_{0, \max} x_{0, \max}' = 1.25 \pi \text{ cm rad}. \quad (2)$$

The maximum energy spread is found from Eq. (1) as:

$$\left(\frac{\Delta p}{p_0}\right)_{\max} = \frac{a}{R+L} = 0.15. \quad (3)$$

In the vertical direction, particle motion is unaffected except edge defocusing at the entrance and exit of the bending magnets. The maximum vertical slope of particle trajectory including edge defocusing is $y_{0, \max}' = 0.027$, and maximum initial vertical displacement of the positrons is $y_{0, \max} = 0.9$ cm. Therefore, vertical acceptance is

$$\epsilon_y = \pi y_{0, \max} y_{0, \max}' = 0.024 \pi \text{ cm rad}. \quad (4)$$

Applying above constraints to the initial positron distribution, it was found that the value of positron transmission efficiency has a maximum of $\Delta N/N = 10^{-2}$ for particle energy of 6 MeV.

An additional feature of the double 90° magnets design is absence of the depolarization of positrons. Spin precession of positrons with the anomalous magnetic moment $G = 0.001159652$ in a 90° bending magnet is:

$$\varphi = \theta \gamma G = 90^\circ \times 20 \times 0.00116 = 2^\circ. \quad (5)$$

However, spin rotation in the first bending magnet is compensated by the second magnet.

Transmission efficiency in the spectrometer is improved by inserting a solenoid between the positron production target and the bending magnets. The focusing properties of the solenoid lens are characterized by the focal length of the lens, f , defined as

$$\frac{1}{f} = \left(\frac{e}{2p_z}\right)^2 \int_{-d}^d B_z^2 dz \quad (6)$$

where B_z is the longitudinal on-axis component of the magnetic field of the solenoid. As far as positron momentum $p_z = eBR$, where B is the bending field, there is a linear relationship between the values of B and B_z to provide optimal focusing of particles along the beamline. An increase of the bending field, to provide transmission of positrons with larger energy, requires a proportional increase of the solenoid field.

RESULTS OF SIMULATION

The proposed spectrometer is characterized by large values of $x/R \sim 0.4$ and momentum deviation $\Delta p/p \sim 0.15$. The linear model based on matrix multiplication is not sufficient to provide accurate estimations of positron dynamics in the spectrometer. For calculation, the code BEAMPATH was used. Particle tracking was accompanied with integration of the Thomas-BMT equation, describing the precession of the spin vector \vec{S} :

$$\frac{d\vec{S}}{dt} = \frac{e\vec{S}}{m\gamma} \times \left[(1+G\gamma)\vec{B}_\perp + (1+G)\vec{B}_\parallel + \left(G\gamma + \frac{\gamma}{1+\gamma} \right) \frac{\vec{E} \times \vec{\beta}}{c} \right], \quad (7)$$

where \vec{E} is the electrical field, and \vec{B}_\perp and \vec{B}_\parallel are components of the magnetic field perpendicular and parallel to particle velocity. Initially, the spin vector of each positron is pointed along the momentum vector. During beam transport, the spin vector precesses. We define the longitudinal polarization as an average of the product of the longitudinal component S_z and the value of polarization, P , summed over all positrons:

$$\langle P_z \rangle = \frac{1}{N} \sum_{i=1}^N S_z^{(i)} P^{(i)}. \quad (8)$$

The initial value of longitudinal polarization is $\langle P_z \rangle = 0.41$. After removing low-energy positrons in the spectrometer, the polarization of the final beam can reach the value of 0.8.

Particle trajectories in the proposed system are presented in Fig. 7. Fig. 8 contains transmission and polarization of positrons in the proposed spectrometer as a function of particle energy. The appearance of the positron transmission maximum is explained by the fact that low energy positrons are strongly divergent and only a small fraction of positrons is within the transverse acceptance of the spectrometer. With increasing energy, the positron beam becomes less divergent, but the number of positrons drops.

At the entrance and at the exit of the magnet, the slope of the particle trajectory is changed because of the pole angle α , according to the linear matrix transformation $\Delta x' = (x/R)\text{tg}\alpha$, $\Delta y' = -(y/R)\text{tg}(\alpha - \psi)$, where the correction angle ψ is given by

$$\psi = K_1 \left(\frac{g}{R} \right) \left(\frac{1 + \sin^2 \alpha}{\cos \alpha} \right) \left[1 - K_1 K_2 \left(\frac{g}{R} \right) \text{tg}\alpha \right], \quad (9)$$

where g is the gap of the magnet and coefficients K_1 , K_2 are defined by pole geometry. For $\alpha = 0$, the value of angle $\psi = 16^\circ$. Selecting $\alpha = 16^\circ$ (horizontal edge defocusing), the value of the correction angle in this case, according to Eq. (9) is $\psi = 11.5^\circ$ and the total effect in vertical direction is focusing $\alpha - \psi = 4.5^\circ$. Fig. 9 illustrates positron transmission as a function of pole face rotation angle. The value of transmission efficiency has a maximum around $\alpha = 16^\circ$.

Fig. 10 illustrates transmission efficiency as a function of field index.

$$n = - \left[\frac{R}{B} \frac{\partial B}{\partial x} \right]_{x=0, y=0}. \quad (10)$$

Positron transmission efficiency has a maximum at the value of $n = 0.4$. In this case focusing properties of the bending magnets are approximately equal each other in both directions. This value of field index was selected for final design.

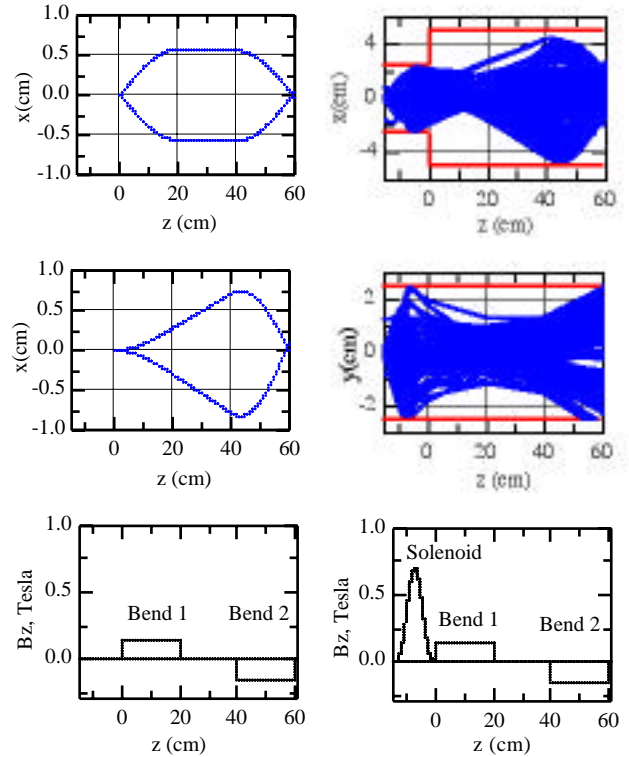


Figure 6: Particle trajectories in spectrometer: (up) $dx/dz = \pm 0.05$, (bottom) $\Delta p/p = \pm 0.02$.

Figure 7: Particle trajectories in the spectrometer.

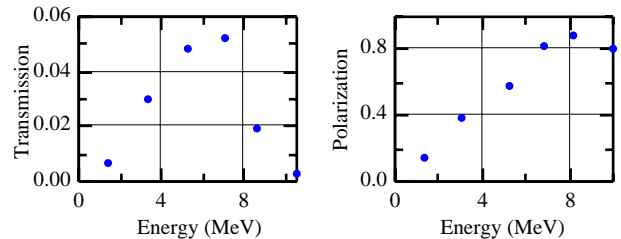


Figure 8: Positron transmission and polarization as functions of energy.

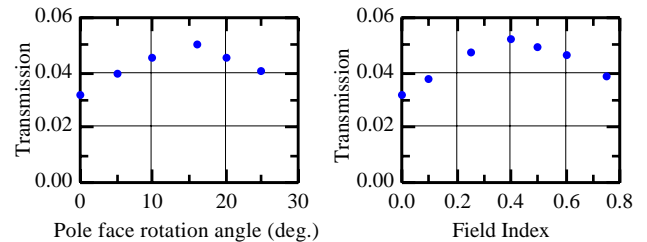


Figure 9: Positron transmission as a function of pole face rotation angle.

Figure 10: Positron transmission as a function of field index.

REFERENCES

- [1] "Undulator-based production of polarized positrons. A proposal for the 50-GeV beam in the FFTB", SLAC-NT-04-018, (20004), 67 pp.
- [2] W.Nelson, H.Hirayama and D.Rogers, "The EGS4 Code System", SLAC-Report-265 (1985).
- [3] K.Flottmann, Ph.D. Thesis, DESY-93-161A (1993).